Published in IET Science, Measurement and Technology
Received on 15th December 2009
doi: 10.1049/iet-smt.2010.0011

ISSN 1751-8822

Analog detection device in a sub-micron linear encoder based on a fibre-optic interferometer with a 3×3 coupler

H.W. Chow N.C. Cheung W. Jin

Department of Electrical Engineering, The Hong Kong Polytechnic University, Hung Hom, Kowloon, Hong Kong
E-mail: eencheun@polyu.edu.hk

Abstract: This study demonstrates a high-resolution linear incremental encoder for high-precision feedback control loop. This novel encoder uses a fibre-optic interferometer with a 3 × 3 coupler and a signal comparator circuit to generate quadrate encoding output signals for the displacement measurement of the moving object. The encoder should be able to achieve a resolution of 95.5 nm and a measurement accuracy of ±0.38 μm.

1 Introduction

Recently, control of a high-precision system is being highlighted in industrial area as the product size become smaller and smaller. Accurate displacement sensors are needed to provide position information for implementing a feedback control. Engineers are working hard in developing precision sensors such as infrared reflective sensor for submicron-level [1], high-precision magnetic grid displacement sensor with resolution down to sub-micron [2] and sensorless measurement method with electromotive force and position observer [3].

One of the most conventional displacements sensing method may be using the linear optical encoder [4]. An encoder generates two quadrate square waves (phase A and phase B) when the sensor is moving. By counting the number of pulse of each phase and measuring the relation between phases A and B (leading and lagging), the moved distance and direction can be determined. This encoding method is widely adopted and decoders are usually available in commercial digital signal processors (DSPs).

A fibre-optic interferometer with a 2 × 2 coupler is another type of displacement sensor that has been used in displacement measurement. The precision of the interferometric displacement sensors depend on the optical wavelength λ, which can be brought down to sub-micron (even down to nanometre and picometre) level. Engineers have proposed and/or developed high-precision and high-resolution displacement sensors based on optical interferometric method. For example, a self-mixing laser sensor with Kalman filter is designed to measure the frequency response of a plate with passive damping [5], a Michelson interferometer with fibre Bragg grating and wavelength-division-multiplexing technique is used for high-stability displacement sensor construction [6]. A quadrature phase-shift interferometer displacement sensor is generating two sinusoidal waves, which could be decoded by conventional analog incremental decoding method [7, 8]. Although high precision could be obtained by using an interferometer with a 2 × 2 coupler, this type of interferometer requires delicate light beam alignment, external optical components and electronic designs to extract the direction information.

An interferometer with 3 × 3 coupler proposed by Sheem in 1980 [9, 10] could overcome this problem. This advanced 3 × 3 coupler is able to generate the direction information. Since interferometric sensors with 3 × 3 coupler does not require many extra fibre-optic components and electronics to extract direction information, it is relatively simple and easy to implement as compared with sensors based on 2 × 2 couplers. On the basis of theory proposed by Sheem, a low coherence displacement sensor with 3 × 3 interferometer (interferometer with a 3 × 3 coupler) was

constructed [11]. However, this low coherence displacement sensor is only able to perform measurement over a very short distance.

Another 3 × 3 interferometric displacement sensor is proposed in [12], and this sensor uses a laser to achieve a longer measurement range; however, the measurement speed is less than 1 mm/s and not suitable for real-time feedback control. In this paper, signals from interferometer outputs are processed so that higher resolution can be achieved. By combining the high-precision 3 × 3 optical interferometer and a dedicated analog signal processing circuit, a linear incremental encoder with long measurable range and improved measurable speed have been demonstrated.

2 Overall system design

Fig. 1 shows the overall design of the proposed displacement sensor. It consists of four main sections, which are the optical circuit, the intensity to voltage conversion, the electric signal processing circuit and the DSP. The optical circuit generates the displacement information related to position of moving targets. This information is given in terms of optical intensities and is converted into electric signals by intensity-to-voltage conversion. The electric signals carrying displacement information are then processed by the electric circuit to achieve incremental encoding. Outputs of the electrical circuit are two quadrate square waves (phases A and B) and they are suitable for information extraction by general incremental decoding. Note that the DSP is responsible for calculating DC offsets of the outputs of interferometer. Offset calculation is updated at 10 Hz by the DSP.

3 3×3 optical interferometer

The optical interferometer used in this proposed sensor is constructed by a passive optical component called 3 × 3 optical coupler. The detail configuration of optical interferometer is shown in Fig. 2.

Light from a laser is coupled into the input port of a 3 × 3 optical coupler through an optical isolator. The light beam is split into three equal intensity light beams, which are, respectively, denoted as P_1, P_2 and P_3 as shown in Fig. 2. P_1 is not used in this design. P_2 is reflected by a reference

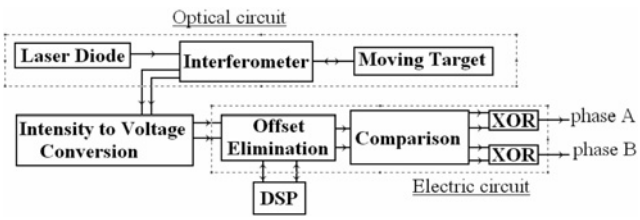

Figure 1 *Overall design of proposed sensor*

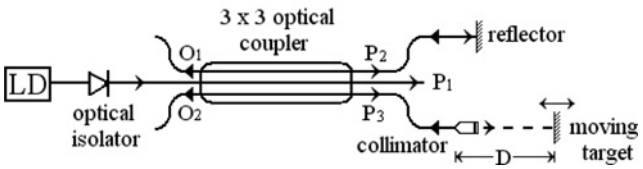

Figure 2 *3 × 3 optical interferometer*

reflector and P_3 leaves the fibre and reflected back by moving surface. Obviously, the optical path difference between P_2 and P_3 depends on distance D, which is between collimator and mirror. Reflected signals of P_2 and P_3 interfere at the coupler, and the interferometer output signals O_1 and O_2 as functions of D are shown in Fig. 3. Therefore the position of mirror could be obtained by measuring the interferometer output signals. The O_1 and O_2 in Fig. 3 are based on (1). These optical power output equations have been proven by Sheem in [9] and [10]

$$|E_{O_1,O_2}(\phi, L_{lc})|^2 = \frac{1}{18}B^2[(7 + 2\cos 3KL_{lc}) - 2\cos\phi(1 - \cos 3KL_{lc}) \pm 6\sin\phi \sin 3KL_{lc}] \quad (1)$$

Variable ϕ in (1) is given in (2). B is a constant and it is related to amplitudes of optical signals P_2 and P_3 from the 3 × 3 coupler. L_{lc} is the length of the coupler and K is the coupling coefficient within the waveguides of the coupler

$$\phi = \frac{4\pi}{\lambda}(L_3 - L_2) + \frac{4\pi D}{\lambda} \quad (2)$$

In (2), L_2 is the fibre length travelled by P_2 and L_3 is the fibre length travelled by P_3. λ is the wavelength of the laser.

4 Signal encoding method

Chow *et al.* [12] proposed an interesting idea to generate conventional incremental encoder outputs from

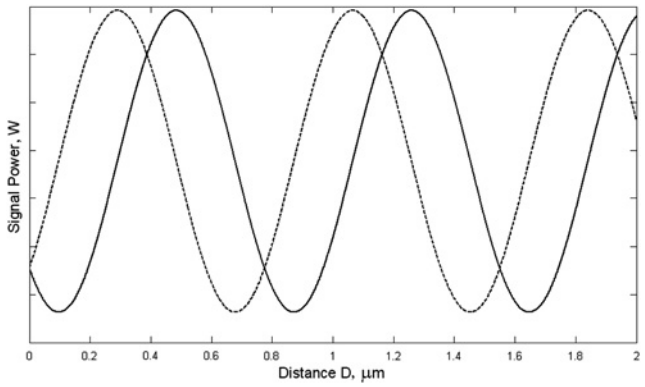

Figure 3 *Outputs of interferometer O_1 and O_2*

Note that *x*-axis is the distance between collimator and moving target and it assumes $L_3 = L_2$

doi: 10.1049/iet-smt.2010.0011

interferometer output signals. This idea can also improve the resolution of the interferometric displacement sensor discussed here and provide quadrature pulses for conventional incremental encoding.

When the reflecting surface as shown in Fig. 2 moves away from fibre with a constant velocity (e.g. 1 mm/s), the two optical output signals (O_1 and O_2) vary periodically as shown in Fig. 4*a*. The DC offsets of the signals from O_1 and O_2 are then removed and the offset-removed signals are named signals x and y. Based on signals x and y, four analog outputs (LC signals) are produced using the following linear combinations (LC)

$$\begin{aligned} &\text{LC1:}y - x \\ &\text{LC2:}y + x \\ &\text{LC3:}2y + x \\ &\text{LC4:}y + 2x \end{aligned} \tag{3}$$

These LC signals are further converted or digitalised to square wave formats by comparing LC signal with zero. The aforementioned LC operation and digitising can be achieved by simple electronic comparator circuits. Four digital signals (the comparator outputs) corresponding to LC1 to LC4 are shown in Fig. 4*b*. If XOR gates are applied between LC outputs (i.e. phase A is LC1 ⊕ LC2 and phase B is LC3 ⊕ LC4), the resolution of the sensor could be further improved. The outputs of XOR gates are shown in Fig. 4*c*. By using phases A and B as decoding signals, eight clock pulses can be generated by decoder for a displacement of $\lambda/2$ (the interferometer is working in a reflection mode). Hence, the sensor resolution may be calculated as $\lambda/16 = 95.5$ nm, where λ is the wavelength of the laser source.

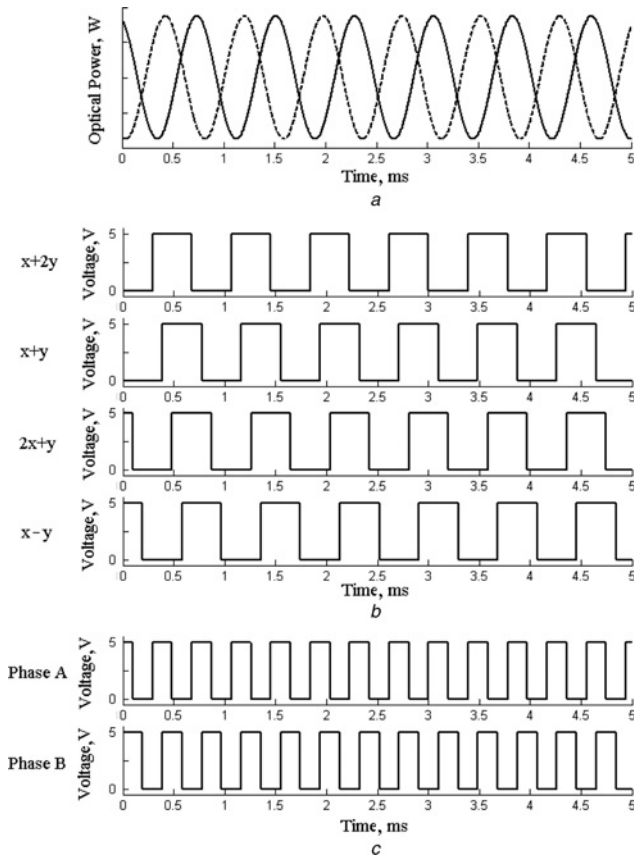

Figure 4 *Simulation for output signal of proposed processing in time domain*

a Optical outputs of interferometer
b Linear combination signals defined in (3) in digital form
c Final outputs of proposed sensor

5 Measurement speed improvement

In [12], the signal processing mentioned in Section 4 is achieved by DSP. However, a typical DSP might not be fast enough for waveform acquisition and this will cause signal distortion if the object is moving at a high speed. This is because a high-speed movement of the object would result in higher frequency optical signal waveforms and they would be distorted if the sampling speed is not sufficiently high. The sampling time of a typical DSP system is about 0.1 ms, corresponding to a sampling frequency of 10 kHz. To restore the signal, the minimum number of sampling points per cycle needs to be eight, since there are eight crossing points as shown in Fig. 5. That means that the maximum speed of the moving subject is $1/(0.0001 \times 8) \times (\lambda/2) = 0.969$ mm/s. Obviously, this speed is far too low for real-time feedback control. Therefore this paper proposes a novel signal conditioning

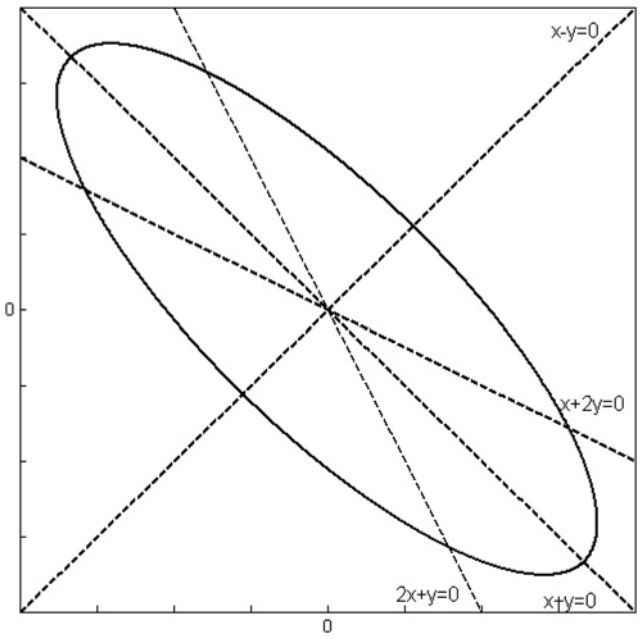

Figure 5 *Lissajous figure with offset-removed signals x and y*

Note that dotted lines represent the conditions for comparison

analog circuit so that the distortion problem could be minimised and the operating speed could be increased. Dedicated comparison function circuit and XOR gates are employed to combat the high-frequency signals and to solve distortion problems.

The use of analog circuits overcomes the speed limitations because of signal sampling and analog to digital conversion. The speed limitation is now solely because of the cutoff frequency of circuits. In demonstration prototype, the 3 dB cutoff frequency is about 150 kHz, which means that the measurement speed can be as high as 10 cm/s.

6 Analog circuit design

A schematic of the proposed analog circuits is shown in Fig. 6. Optical outputs from the interferometer are converted into voltage signals by trans-impedance amplifiers comprising of photo-diodes, resistors, variable resistors and operational amplifiers. Photo-diodes convert the light power (intensity) to photo-currents, which are then amplified and converted to voltages by operational amplifiers. The variable resistors are used for small manual adjustment to produce equal amplitude outputs.

Since the offsets of both optical signals are varying at a very slow rate, the offset detection may be performed by a DSP. Optical signals are inputted to the DSP and their offsets are calculated. The offset of optical signals are updated at frequency 10 Hz since the offset variation is slow. Meanwhile, optical signals are subtracted by their offsets using difference amplifiers. Offset-removed signals x and y are then obtained and used for further processing.

Four comparators are used to perform the operations of linear combination and digitalisation as have been described in Section 4. Signals x and y are firstly amplified to $-x$, $-2x$ and $-2y$ by inverting amplifiers and are inputted into four comparators to generate the digital version of the four linear combination signals ($y-x$, $y+x$, $y+2x$, $2y+x$) as shown in Fig. 4*b*. As mention in Section 3, the resolution can be improved by using two XOR gates as shown in Fig. 6 to generate encoded signals (phases A and B as shown in Fig. 4*c*) with a better resolution.

7 Implementation issues

Ideally, when the object moves at constant speed, the Lissajous figure could be drawn and shown in Fig. 5. If object moves a distance $\lambda/2$, this will be equivalent to a point travelling one ellipse. The travelling time between each crossing point is equal and thus phases A and B can be generated in regular shape. However, in real situation, signals' amplitudes are not identical and their offsets are residue and not zero. This causes the travelling time between crossing points to be different. Phases A and B will be in irregular shape.

7.1 Unequal amplitude effects

Considering the case in which offsets of both signals are zero but their amplitudes are unequal, the performance of encoder is illustrated by Fig. 7*a*. Although the shape of Lissajous figure is distorted, the ellipse can still pass through four lines (i.e. eight crossing points). Travelling time between two intersection points is different. Phases A and B will be distorted and shown in lower part of Fig. 7*a*. Nevertheless, as long as the ellipse crosses four linear combination lines, the maximum error is limited to $\lambda/4$.

7.2 Residue offset signal effects

Considering the case that offsets of both signals are not zero but their amplitudes are equal, the effect of encoder performance is illustrated by Fig. 7*b*. Obviously, the ellipse cannot cross all four lines and that means number of square waves generated by analog circuits are not able to reflect the displacement information. The error in displacement measurement will accumulate and become larger and larger.

7.3 Minimisation of unwanted effects

The effect of unequal amplitude can be minimised by using a variable resistor within the trans-impedance amplifier to adjust and minimise the difference between amplitudes of two signals from the interferometer outputs.

For non-zero signal offset, offset detection and elimination circuits shown in Fig. 6 have already minimised the effect. However, small residue offsets may still exist. If the offsets are not as serious as shown in Fig. 7*b* such that the ellipse

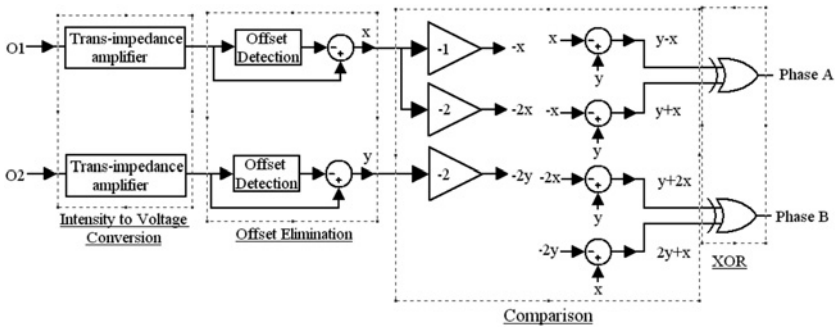

Figure 6 *Schematic of the electric circuit*

doi: 10.1049/iet-smt.2010.0011

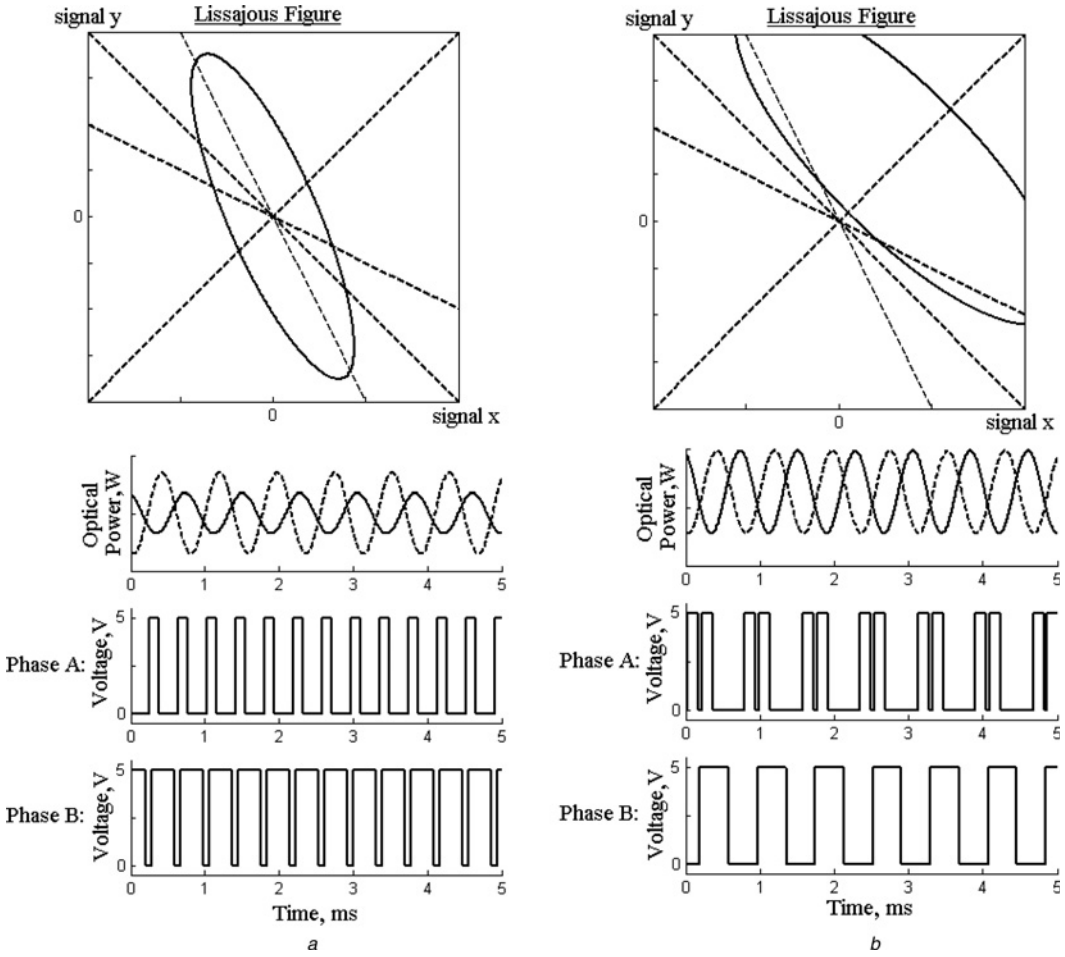

Figure 7 *Demonstration of proposed sensor outputs*

a Amplitudes of offset-removed signal are different
b Offsets of signals are different

still can cross four lines, this performance may still be regarded as acceptable and the measurement errors are bounded to $\lambda/4$.

8 Experimental setup and result

Fig. 8 shows the schematic of the experimental system used to verify the performance of the proposed incremental encoding displacement sensor. Several important points regarding the experiment setup should be mentioned. The 2×2 coupler is used to form a fibre-loop reflector [13], which performs the role of a reflector as shown in Fig. 2. The moving target (mirror) is installed on a controlled voice coil motor (VCM), which is oscillated and driven by constant voltage source and H-bridge controller. The variable resistor within the trans-impedance amplifier is used for small manual adjustment to compensate difference in amplitudes. DSP is responsible for offset detection (offset updating rate is 10 Hz) and converting phases A and B to displacement by a build-in decoder. In addition, the VCM's position is also measured by a reference sensor (linear optical incremental encoder). Specifications and models of equipments adopted in this experiment are shown in Table 1.

The experimental results shown in Fig. 9 and its details are shown in Fig. 10. The displacement measured by both the proposed and the reference sensors are recorded and the results are shown in the top panels. Note that all the position-time graphs actually contain two curves, which are measured by the two sensors, and the difference is too small to be seen in these top panels because of the large scale used. The difference (error) between two curves is instead shown in the bottom panels. The velocity and acceleration signals shown in the figures are calculated from the position signal of the reference sensor.

9 Accuracy analysis

The measurement errors may be categorised into three types as indicated in Fig. 10. 'Error 1' is about 380 nm $\simeq \lambda/4$. It is obvious that 'Error 1' appeared during the whole process. This error is caused by non-zero offset and differential amplitude that has been explained in Section 7.

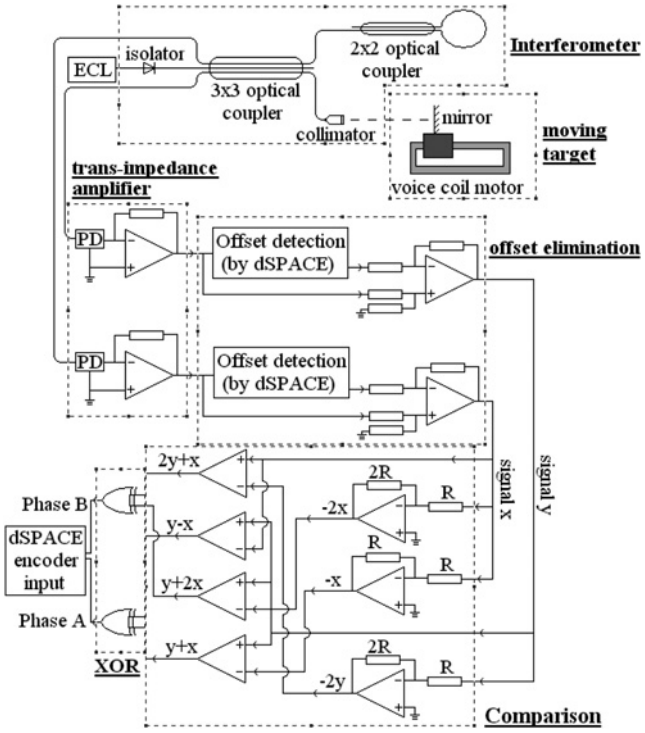

Figure 8 *Experiential setup for proposed sensor demonstration*

'Error 2' and 'Error 3' are found because of the mounting of reflecting mirror. 'Error 2' is caused by the bending of mirror holder during acceleration. Referring to the setup photograph shown in Fig. 11, when current is injected to

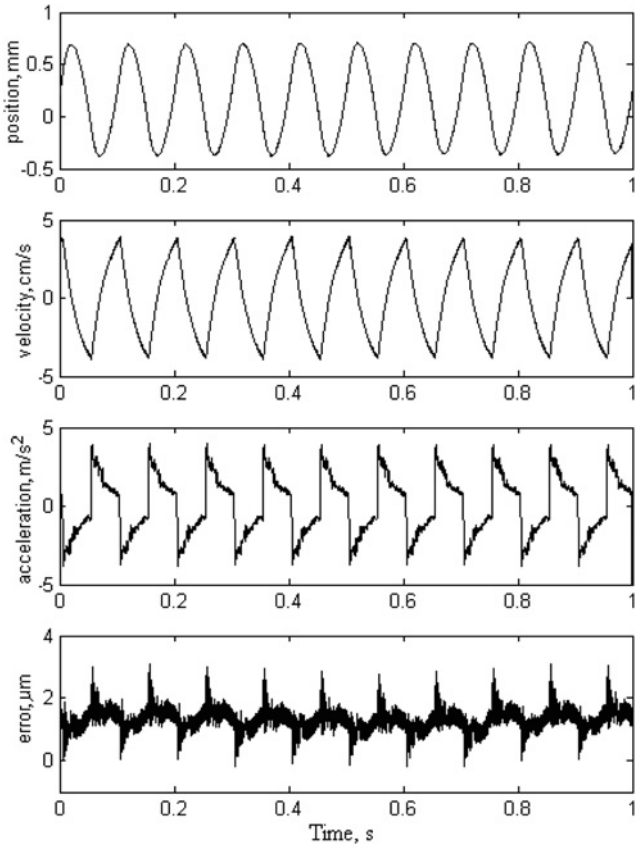

Figure 9 *Experimental result with VCM*

Table 1 Specifications and model of experiment equipments

Name of equipment	Company	Model	Other specification
external-cavity laser (ELC)	new focus	6262	line-width 5 MHz at wavelength = 1550 nm
1550 nm single mode standard 3 × 3 coupler	Go4fiber	SSS-3 × 3–15-33/33/33-Q-9-1	
1550 nm dual-stage optical isolator	Go4fiber	GISD-P-15-9-10-00	
1550 nm standard 2 × 2 coupler	Go4fiber	SSS-2 × 2-15-50/50-Q-9-1	
PCB wiring-head-machine (VCM)	ASM		maximum acceleration = 5 m/s^2, maximum continue current = 5 A
InGaAs PIN photodiode	Go4fiber	GT322D-A-FC	
DSP board	dSPACE	DS1104 R&D controller board	
operational amplifiers	analog device	OP37	
comparators	national semiconductor	LM339	
XOR gates	texas instruments	SN74ACT86N	
linear optical incremental encoder	Renishaw	RGH24H30D30A	50 nm resolution

doi: 10.1049/iet-smt.2010.0011

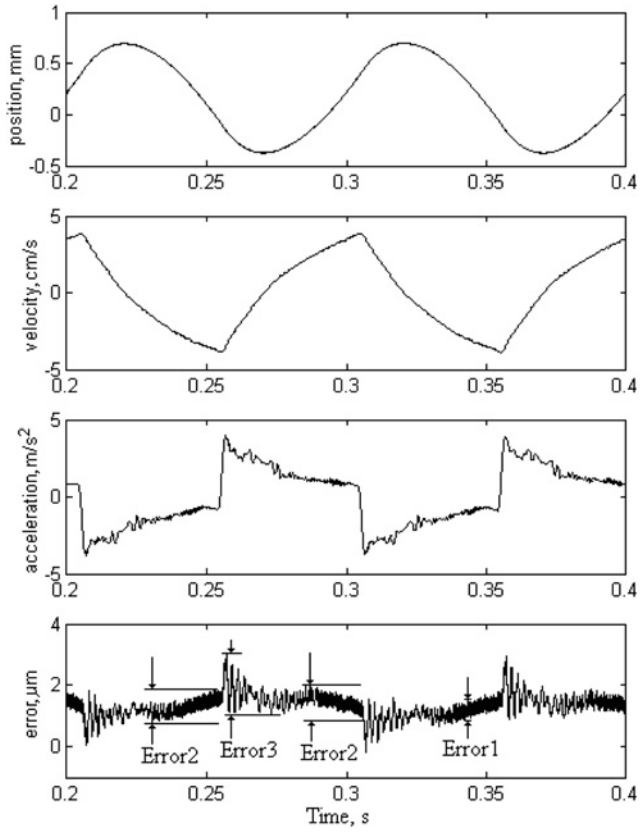

Figure 10 *Detail of experimental result (between 0.2 and 0.4 s)*

the VCM, the mover of VCM and the 'L'-shaped metal (incremental encoder ruler is under the 'L'-shaped metal) shown in Fig. 11*a* is being accelerated. The attached mirror mount is exerted a torque from the base. Although the material of mirror holder is rigid, springs that could be extended by three screws (shown in Fig. 11*b*) are elastics. This structure is designed for the purpose of optical alignment and allows manual tuning of 'tilt' angle of the mirror by $\pm 7^{\circ}$. The elastic properties of springs will also result in unwanted 'tilt' of the mirror during the acceleration process. The tilt angle has opposite signs for acceleration in the opposite directions and it is equivalent to a change of the mirror position and results in 'Error 2'.

'Error 3' appears when the object changes its direction. This is because the change of direction causes a sharp change in the acceleration (Fig. 10, the second last panel), which exerts a 'step-like' force to the spring-supported system and causes the mirror holder to oscillate relative to the base. The reflecting mirror picks up this oscillation whereas the reference sensor does not because it is attached to the base where the mover of VCM is located. The difference between two measurements is then the 'Error 3'. To further verify this explanation, another experiment was performed with slow change of acceleration and the result is shown in Fig. 12. In this experiment, there is no sharp change in acceleration and 'Error 3' disappears. To conclude, 'Error 2' and 'Error 3' are related to mechanical property of the mirror holder and could be avoided or reduced by proper mechanical design of the mirror mounting.

Although presented experiments were performed with an external cavity laser, in a practical system, it may be replaced by a lower-cost distributed feedback laser (DFB). By locking to a gas absorption line, the frequency of the DFB laser can be stabilised with r.m.s. deviation equal to or smaller than 50 MHz, which is ~0.4 pm in terms of wavelength variation [14, 15]. Assuming a maximum single-way path difference of $D = 10$ cm, the resulting

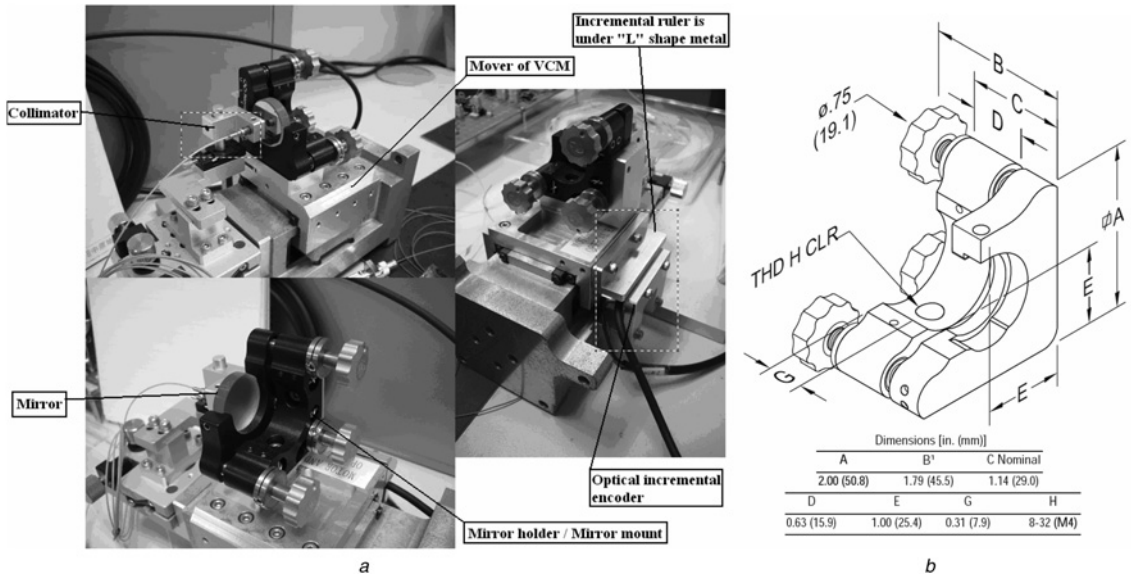

Figure 11 *Mover of VCM, the reflecting mirror and optical incremental encoder*

a Photographs of the instruments
b Mechanical drawing together with dimension of mirror mount

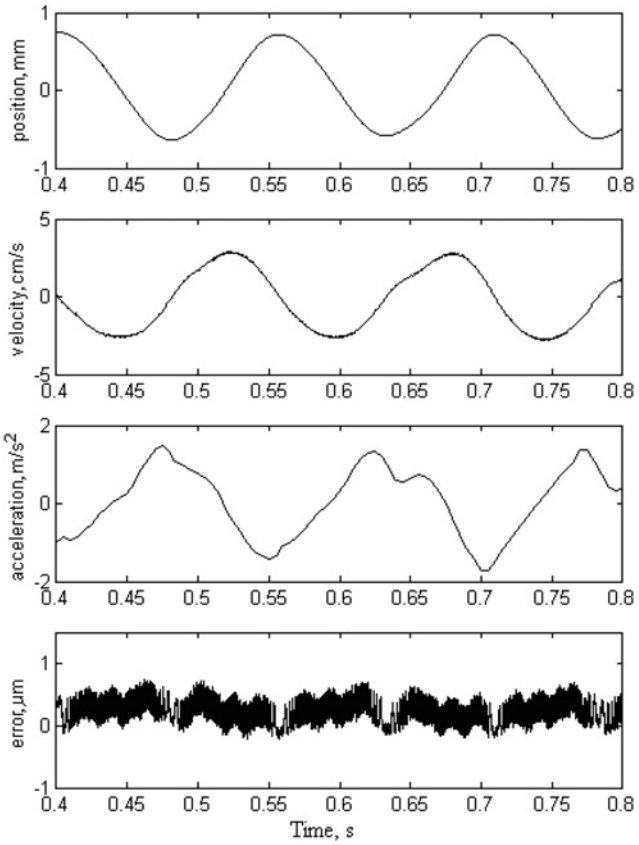

Figure 12 *Experimental result with VCM driven under small acceleration*

phase change is given by $4\pi D\delta\lambda/\lambda 2 = \sim 2.2$ rad, or a displacement error is 0.26 μm, which is smaller than $\lambda/4$.

10 Conclusions

A high-precision incremental encoder sensor based on 3 × 3 interferometer and a high-coherent laser is proposed and verified experimentally. The displacement measurement is achieved through signal conversion from outputs of 3 × 3 interferometer into quadrate square waves. The resolution of the sensor is 95.5 nm. The measurement deviation of proposed sensor is $\sim \pm 0.38$ μm. The signal processing and encoding are achieved by dedicated analog circuits so that the measurement speed can be up to 10 cm/s. The speed is limited by present hardware, which is general-purpose operational amplifier and its range could be extended to tens of meter per second by increasing the cutoff frequency of the electronic circuits in the MHz range.

The external cavity laser used in the present setup may be replaced by a DFB laser together with a gas cell for wavelength stabilisation. The use of DFB laser would allow a system with a much lower cost and similar accuracy and measurement range. The precision of the sensing system may be further improved by using a shorter wavelength laser.

The proposed method is especially suitable for ultra-high-precision dynamic displacement measurement, such as the feedback control of linear servo motors.

11 Acknowledgment

The author thanks the Hong Kong Polytechnic University for the support of this project through research account RP47.

12 References

[1] CHEN Z., YAO B., WANG Q.: 'Desired compensation adaptive robust control of a linear-motor-driven precision industrial gantry with improved cogging force compensation', *ASME Trans. Mechatron.*, 2008, **13**, (6), pp. 617–624

[2] HAO S.H., LIU J.Z., HAO M.H., SONG B.Y.: 'Design of high precision magnetic grid displacement sensor'. Proc. 2008 IEEE Int. Conf. on Mechatronics and Automation, 5–8 August 2008, pp. 185–188

[3] LEIDHOLD R., MUTSCHLER P.: 'Sensorless position-control method based on magnetic saliencies for a Long-Stator Linear Synchronous-Motor'. IECON 2006 – 32nd Ann. Conf., 6–10 November 2006, pp. 781–786

[4] RIEDER H., SCHWAIGER M.: 'Linear incremental measuring system for measuring speed and displacement'. United States Patent, Patent number: 4716292, 29 December 1987

[5] BES C., BELLOEIL V., PLANTIER G., GOURINAT Y., BOSCH T.: 'A self-mixing laser sensor design with an extended Kalman filter for optimal online structural analysis and damping evaluation', *ASME Trans. Mechatron.*, 2007, **12**, (3), pp. 387–394

[6] LU Y., XIE F., WU S.: 'On-line displacement measurement using a high stability multiplexed optical fiber interferometer system'. 2008 Second IEEE Int. Nanoelectronics Conf. (INEC 2008), pp. 1159–1161

[7] MURPHY K.A., GUNTHER M.F., VENGSARKAR A.M., *ET AL.*: 'Quadrature phase-shifted, extrinsic Fabry–Perot optical fiber sensors', *Opt. Lett.*, 1991, **16**, (4), pp. 273–275

[8] MURPHY K.A., GUNTHER M.F., VENGSARKAR A.M., *ET AL.*: 'Extrinsic fiber optic displacement sensors and displacement sensing systems'. United States Patent, Patent number: 5301001, 5 April 1994

[9] SHEEM S.K.: 'Fiber-optic gyroscope with 3 × 3 directional coupler', *Appl. Phys. Lett.*, 1980, **37**, pp. 869–871

[10] SHEEM S.K.: 'Optical fiber interferometers with 3×3 directional couplers: analysis', *J. Appl. Phys.*, 1981, **52**, pp. 3865–3872

doi: 10.1049/iet-smt.2010.0011

[11] TOMIC M.C., ELAZAR J.M., DJINOVIC Z.V.: 'Low-coherence interferometric method for measurement of displacement based on a 3 × 3 fibre-optic directional coupler', *J. Opt. A: Pure Appl. Opt.*, 2002, **4**, pp. S381–S386

[12] CHOW H.W., CHEUNG N.C., JIN W.: 'A low cost sub-micro linear incremental encoder based on 3 × 3 fiber-optic directional coupler', *IEEE Trans. Instr. Meas.*, 2010, **59**, pp. 1624–1633

[13] MORTIMORE D.B.: 'Fiber loop reflectors', *J. Lightwave Technol.*, 1988, **6**, (7), pp. 1217–1224

[14] CLICHÉ J.-F., ZARKA A., TETU M., CHARTIER J.-M.: 'Automatic locking of a semiconductor laser at -633 nm on linear absorption iodine transitions', *IEEE Trans. Instr. Meas.*, 1999, **48**, (2), pp. 596–599

[15] CLICHÉ J.-F., TETU M.: 'Automatic absolute frequency calibration of tunable optical sources'. Optical Fiber Communication Conf. 2000, 7–10 March 2000, vol. 2, pp. 269–271